Optical bistability in shape-memory nanowire metamaterial array

Yusuke Nagasaki[1, 2], Behrad Gholipour[1, 3], Jun-Yu Ou[1, a)], Masanori Tsuruta[1,4], Eric Plum[1], Kevin F. MacDonald[1], Junichi Takahara[2, 5] & Nikolay I. Zheludev[1, 6]

[1]Optoelectronics Research Centre and Centre for Photonic Metamaterials, University of Southampton, Highfield, Southampton, SO17 1BJ, UK.

[2]Graduate School of Engineering, Osaka University, 2-1 Yamadaoka, Suita, Osaka 565-0871, Japan.

[3]Department of Chemistry, University of Southampton, Highfield, Southampton, SO17 1BJ, UK.

[4]Asahi Kasei, Energy and Environment R&D Center, 2-1 Samejima, 416-8501, Fuji, Japan.

[5]Photonics Advanced Research Center, Osaka University, 2-1 Yamadaoka, Suita, Osaka 565-0871, Japan.

[6]Centre for Disruptive Photonic Technologies, SPMS, TPI, Nanyang Technological University, Singapore 637371, Singapore.

Abstract

Non-volatile temperature-induced structural phase transitions such as those found in chalcogenide glasses and chalcogenide-based nanostructures are known to lead to strong changes in their optical properties and are widely used in rewritable optical disk technology. Here, we demonstrate that thermally-activated optical memory can be achieved with a metallic nanowire array made from a shape-memory alloy. A nickel-titanium film of nanoscale thickness structured on the subwavelength scale exhibits bistability of its optical properties upon temperature cycling between 30°C and 210°C. The structure, which consists of an array of NiTi nanowires covered with a nanoscale thickness gold layer to enhance its plasmonic properties, can exist in two non-volatile states presenting an optical reflectivity difference of 12% via nanoscale mutual displacements of alternating nanowires in the structure. Such all-metal shape memory photonic gratings and metamaterials may find applications in bistable optical devices.

---

a) Author to whom correspondence should be addressed: jo2c09@orc.soton.ac.uk

Structuring of materials on length scales comparable to or smaller than the wavelength of electromagnetic radiation enables the design of metamaterials, photonic crystals and gratings with optical properties that are enhanced or different from those available from natural materials.[1,2] Periodically structured surfaces may be referred to as metamaterials or metasurfaces when they interact with radiation that has a wavelength longer than said period. In respect to shorter wavelengths of radiation, the same structures are diffractive gratings. Several approaches for tuning, modulating and switching the functionalities of such structured materials have emerged, including (i) mechanical actuation of the internal structure of metamaterials,[3–9] (ii) inclusion of phase-change media (e.g. chalcogenide glasses, vanadium dioxide, gallium)[10–12] or nonlinear materials[13], and (iii) all-optical 'coherent control' of the interaction of ultrathin metamaterials with light.[14] Here we introduce a reconfigurable photonic nanostructure which exhibits optical memory behaviour underpinned by the shape-memory effect. Shape-memory alloys are binary or ternary metallic alloys that exhibit thermally-induced reversible transitions between structural phases with different mechanical properties. Temperature-activated shape-memory effects were first observed in gold-cadmium alloys[15, 16] and became widely used with the discovery of nickel-titanium alloy,[17, 18] leading to a variety of applications ranging from actuators and valves to stents.[19, 20]

To demonstrate thermally-activated optical memory with a shape-memory alloy we developed a nanostructure, an array of nickel-titanium (NiTi) nanowires supported on silicon nitride nano-beams and covered with a gold layer of nanoscale thickness (Figure 1). The purpose of the plasmonic gold layer is to enhance the resonant optical characteristics of the structure while the SiN–NiTi bimorph provides hysteretic temperature-activated reconfiguration of the nanostructure that leads to non-volatile changes of the composite's optical properties. The NiTi alloy was chosen as the active memory agent because it retains shape-memory properties at the nanoscale.[21, 22] The beams of the array are anchored to the unstructured part of the membrane and every second beam of the array has trenches cut through the gold into the NiTi layer at either end close to the anchor points (see inset to Figure 2). Temperature variations cause stress in the beams due to differential expansion of the constituent layers. The stress causes a larger deformation of weakly anchored beams (with trench cuts) than robustly anchored beams (without). As the optical properties of the array are sensitive to the mutual positions of the beams, a change in temperature leads to a change of the array's optical properties. The central NiTi shape-memory alloy layer of the structure undergoes a hysteretic transition between martensite and austenite solid phases upon temperature cycling. This leads to a hysteresis in the thermal expansion that drives beam deformation, in turn giving rise to hysteretic changes in the optical properties of the array during a temperature cycle.

The shape-memory nanowire array was manufactured on a silicon nitride (SiN) membrane by sputtering of NiTi alloy, thermal evaporation of gold and subsequent nanostructural patterning by focused ion beam milling. 175 nm of NiTi (42% Ni, 58% Ti) was deposited on a commercially sourced SiN membrane of 50 nm thickness by radio-frequency sputtering (Kurt J. Lesker Nano 38) from 99.999% purity NiTi and Ni targets (Testbourne), providing for accurate control over the deposited film's composition.[22-24]. A base pressure of 4.0×10^{-5} mbar

was achieved before deposition. A flow rate of 10 cubic centimetres per minute (SCCM) of high purity argon was used to strike the plasma on both targets. The substrate was held on a rotating platen with a target-substrate distance of approximately 150 mm, which ensures deposition of low stress films. A working pressure of 2×10^{-3} mbar was achieved during deposition. The sputtering rate was fixed at 3.50 nm/min. The deposited film was subsequently annealed (Jipelec rapid thermal annealer) at 400°C for 30 min in argon at atmospheric pressure[24, 25] with a heating and cooling rate of 50°C/min and 1°C/min, respectively (the annealing chamber having first been purged with Ar for 2.5h to remove air). The final composition of the shape-memory alloy film was determined by energy-dispersive X-ray spectroscopy to be 42% Ni, 58% Ti. The 50-nm-thick gold layer was deposited on top of the shape-memory alloy by resistance evaporation (Edwards Auto 306) with a base chamber pressure of 2.0×10^{-6} mbar at a deposition rate of 0.05 nm/sec. The nanowire pattern was manufactured by focused ion beam milling (FEI Helios NanoLab 600), cutting through the layers to produce an array of 400-nm-wide freestanding suspended beams separated by 100-nm-wide gaps (Figure 2). In order to avoid over-milling the gold layer, the nanowires were first milled from the SiN membrane side. Then, the sample was turned over and the trenches were milled from the gold side, to a depth of 150 nm, at both ends of every other beam, as shown in the inset to Figure 2.

In order to confirm the shape-memory-alloy properties of the NiTi,[21] the temperature dependence of resistance of a 175-nm-thick NiTi control sample deposited on a SiO_2 substrate was measured. A 4-probe measurement (Keithley 2636B Sourcemeter) was performed under vacuum at a pressure of 4.0×10^{-6} mbar to prevent sample oxidation. The probes were fixed to the sample with conductive adhesive to prevent separation during temperature cycling, which may otherwise occur due to differential thermal expansion of the sample substrate and probes. Upon temperature cycling between ~ 30°C and 220°C, the resistance shows a clear hysteresis loop, which is a characteristic feature of the martensite-to-austenite phase transition for this alloy (Figure 3). This behaviour is maintained through repeated temperature cycling (tested here up to 7 heating-cooling cycles).

To demonstrate the hysteretic behaviour of the shape memory plasmonic nanostructure's optical properties, reflection spectra were recorded at various points in the heating/cooling temperature cycle using a microspectrophotometer (CRAIC QDI2010) with a 15× objective (numerical aperture 0.28). The nanowire structure was illuminated with light polarized linearly perpendicular to the nanowires. Spectra were recorded with an aperture size of 5 μm × 5 μm (i.e. smaller than the 25 μm × 9.5 μm size of the array).

In the absence of deformation, the structure is a metamaterial for wavelengths longer than 500 nm. However, as differential displacement of every second nanowire doubles the period to 1000 nm, the structure becomes diffracting over the experimental wavelength range (500 nm – 870 nm). In reflective measurements, both illumination of the sample and collection of reflected light occur through an objective with a numerical aperture of 0.28 – giving a maximum angle of incidence for illumination and detection of light equal to 16°. As such the microspectrophotometer does not detect diffracted light from a grating of 1000 nm period at wavelengths greater than 560 nm.

The reflectivity spectrum of the nanostructure shows a local maximum at ~500 nm (Fig 4a inset) corresponding to the lattice mode associated with the nanowire spacing. The increase in reflectivity towards the long wavelength end (870 nm) of the measureable spectral range suggests the presence of another reflectivity maximum at longer wavelength, which may be the lattice mode associated with the 1000 nm spacing of identical nanowires.

To measure the temperature dependence of the nanostructure's reflection properties, it was mounted in a thermostatic sample stage. The stage temperature was varied from 30 to 210°C in 20°C steps, allowing 5 minutes for the system to reach thermal equilibrium at each temperature. The optical properties of the shape-memory nanowire array are found to be strongly temperature-dependent and hysteretic, which is to say that the nanostructure presents different reflection spectra depending on whether it has been heated or cooled to a given temperature.

Figure 4a shows differential reflectivity spectra of the nanowire array after heating (red) and cooling (blue) to a temperature of 110°C, relative to the reflectivity at a reference temperature of 210°C. Figure 4b shows the hysteretic temperature-dependence of reflection at a given wavelength (835 nm). The shape-memory nanowire structure is up to 12% more reflective after cooling to a stage temperature of 110°C (a state the may be denoted a logical "1") as compared to having been heated to the same temperature (logical "0"). Starting at room temperature, the decrease in reflectivity with increasing temperature is consistent with increasing deformation of the nanostructure causing more light to be diffracted. This trend is reversed as the sample is heated above 110°C, implying a gradual phase transition in the NiTi layer. As the nanostructure is cooled, its reflectivity at 835 nm is higher (implying reduced diffraction due to reduced nanowire deformation) than at the same temperature during the heating process, until the reflectivity returns to its original value close to room temperature, indicating that the nanowires have returned to their original state.

We conclude that the observed temperature hysteresis (memory) of optical properties is related to the martensite-austenite cycle in NiTi, which results in the existence of two different stable shapes for the nanostructure. Indeed, finite element analysis (COMSOL Multiphysics) indicates that the mid-point of a nanowire with trenches on either end is displaced out of plane by 105 nm at 110°C when NiTi is in the martensite phase and by 70 nm at the same temperature in the austenite phase (Fig. 4c), while the displacement of nanowires without trenches is negligible (< 5 nm) for both NiTi phases.The simulations assume flat nanowires at room temperature, nanowire ends of fixed position and fixed orientation, and martensite and austenite phases with thermal expansion coefficients of 7×10^{-6} and 11×10^{-6} K^{-1} (Ref. 26), Young's moduli of 28 and 83 GPa, and a Poisson's ratio of 0.33 (Ref. 27). As illustrated in Fig. 1, the change in the shape of the nanostructure leads to a change in its plasmonic response and thus in its optical properties, which are dominated by the gold coating on the NiTi framework.

An additional contribution to the change in the nanostructure's optical response may come from a temperature-dependent change in the optical properties of NiTi.

The shape-memory nanowire array reported here demonstrates how non-volatile memory characteristics can be achieved in reconfigurable metamaterial nanostructures based on bimaterial bridge actuators[6-9]. More generally, shape-memory materials provide a broad range of opportunities for active/adaptive plasmonic devices, metamaterials, gratings and photonic crystals: For example, shape memory materials could be used to add hysteretic switching and memory functionalities to thermally actuated metamaterials[6, 8, 28, 29], which are currently deformed by differential thermal expansion of different materials rather than phase transitions. Two-way shape-memory alloys[19] could enable pronounced thermal switching of photonic structures between two distinct states, even without relying on differential thermal expansion. This could allow the realization of thermally switchable, bistable magnetic metamaterials based on three-dimensional split ring resonators.[28-30] Shape-memory polymers, offering reversible strains of up to 800%[31] and multi-shape memory,[32] could act as elastic shape-memory substrates for gratings, photonic crystals and metamaterials reconfigured by stretching.[5] Furthermore, shape-memory polymers, loaded with nanoparticles to achieve a high refractive index, could even serve as nanoimprint substrates, where imprint in regimes of elastic and plastic deformation[33] could be exploited to create temporary and permanent bas-relief metamaterials and gratings,[34] allowing thermal recovery of the latter.

Our proof-of-principle demonstration highlights the opportunity that shape-memory materials provide for reconfigurable photonic nanostructures. Engineering of optimized devices will require systematic studies to achieve optimal performance of alloy and nanostructure, and investigations of device behaviour over a large number of temperature cycles.

In summary, we demonstrate a shape-memory-alloy-based nanomechanical reconfigurable grating. By introducing a phase-change material to a mechanically reconfigurable nanowire array, we realize a mechanically reconfigurable photonic nanostructure with rewritable memory functionality. We expect that shape-memory gratings and metamaterials will enable advanced photonic functionalities: In principle, they can be programmed by permanent deformation into complex shapes, tuned by reversible actuation driven by thermal, electrical, magnetic or optical control signals, and reset with heat.

This work is supported by Asahi Kasei, the UK's Defence Science and Technology Laboratory (grant DSTLX1000064081), the MOE Singapore (grant MOE2016-T3-1-006) and the UK's Engineering and Physical Sciences Research Council (grant EP/M009122/1). Y. N. is supported by Research Fellowships of the Japan Society for the Promotion of Science (JSPS) for Young Scientists, and by the Interactive Materials Science Cadet Program of Osaka University. Following a period of embargo the data from this paper can be obtained from the University of Southampton ePrints research repository: http://dx.doi.org/10.5258/SOTON/XXXXXX.

1. N. I. Zheludev, Science **348**, 973-974 (2015).
2. A. F. Koenderink, A. Alù, A. Polman, Science **348**, 516-521 (2015).
3. M. Lapine, D. Powell, M. Gorkunov, I. Shadrivov, R. Marqués, and Y. Kivshar, Appl. Phys. Lett. **95**, 084105 (2009).
4. H. Tao, A. C. Strikwerda, K. Fan, W. J. Padilla, X. Zhang, and R. D. Averitt, Phys. Rev. Lett. **103**, 147401 (2009).
5. I. M. Pryce, K. Aydin, Y. A. Kelaita, R. M. Briggs, and H. A. Atwater, Nano Lett. **10**, 4222-4227. (2010).
6. J. Y. Ou, E. Plum, L. Jiang, and N. I. Zheludev, Nano Lett. **11**, 2142-2144 (2011).
7. J.-Y. Ou, E. Plum, J. Zhang, and N. I. Zheludev, Nat. Nanotech. **8**, 252-255 (2013).
8. J. Valente, J.-Y. Ou, E. Plum, I. J. Youngs, and N. I. Zheludev, Appl. Phys. Lett. **106**, 111905 (2015).
9. N. I. Zheludev, and E. Plum, Nat. Nanotech. **11**, 16-22 (2016).
10. T. Driscoll, H.-T. Kim, B.-G. Chae, B.-J. Kim, Y.-W. Lee, N. M. Jokerst, S. Palit, D. R. Smith, M. D. Ventra, and D. N. Basov, Science **325**, 1518-1521 (2009).
11. B. Gholipour, J. Zhang, K. F. MacDonald, D. W. Hewak, and N. I. Zheludev, Adv. Mater. **25**, 3050-3054 (2013).
12. R. F. Waters, P. A. Hobson, K. F. MacDonald, and N. I. Zheludev, Appl. Phys. Lett. **107**, 081102. (2015).
13. M. Lapine, I. V. Shadrivov, and Y. S. Kivshar, Rev. Mod. Phys. **86**, 1093-1123 (2014)
14. J. Zhang, K. F. MacDonald, and N. I. Zheludev, Light Sci. Appl. **1**, e18 **(**2012)
15. G. V. Kurdyumov, L. G. Khandros, Dokl. Akad. Nauk SSSR **66**, 211-214 (1949).
16. L. C. Chang, T. A. Read, Trans AIME **189**, 47-52. (1951).
17. W. J. Buehler, J. V. Gilfrich, and R. C. Wiley, J. Appl. Phys. **34**, 1475-1477 (1963).
18. K. Otsuka, and X. Ren, Prog. Mater. Sci. **50**, 511–678 (2005).
19. K. Otsuka, and C. M. Wayman, Shape memory materials; Cambridge University Press, 1999.
20. J. M. Jani, M. Leary, A. Subic, and M. A. Gibson, Mater. Design **56**, 1078-1113 (2014).
21. S. Miyazaki, Y. Q. Fu, and W. M. Huang, eds. *Thin film shape memory alloys: fundamentals and device applications* (Cambridge University Press, 2009).
22. Y. Q. Fu, S. Zhang, M. J. Wu, W. M. Huang, H. J. Du, J. K. Luo, A. J. Flewitt, and W. I. Milne, Thin Solid Films **515**, 80-86 **(**2006).
23. A. Ishida, A. Takei, and S. Miyazaki, Thin Solid Films **228**, 210-214 (1993).
24. P. Surbled, C. Clerc, B. L. Pioufle, M. Ataka, and H. Fujita, Thin Solid Films **401**, 52-59 (2001).
25. J.-L. Seguin, M. Bendahan, A. Isalgue, V. Esteve-Cano, H. Carchano, and V. Torra, Sensors and Actuators A **74**, 65–69 (1999).
26. J. Uchil, K. P. Mohanchandra, K. G. Kumara, K. K. Mahesh, and T. P. Murali, Physica B **270**, 289-297 (1999).
27. Y. Q. Fu, S. Zhang, M. J. Wu, W. M. Huang, H. J. Du, J. K. Luo, A. J. Flewitt, and W. I. Milne, Thin Solid Films **515**, 80-86 (2006).C. C. Chen, C. T. Hsiao, S. Sun, K.-Y. Yang, P. C. Wu, W. T. Chen, Y. H. Tang, Y.-F. Chau, E. Plum, G.-Y. Guo, N. I. Zheludev, and D. P. Tsai, Opt. Exp. **20**, 9415-9420 (2012).
28. Y. Mao, Y. Pan, W. Zhang, R. Zhu, J. Xu, and W. Wu, Nano Lett. **16**, 7025-7029 (2016).
29. C.-C. Chen, A. Ishikawa, Y.-H. Tang, M.-H. Shiao, D. P. Tsai, and T. Tanaka, Adv. Optical Mater. **3**, 44-48 (2015).
30. W. Voit, T. Ware, R. R. Dasari, P. Smith, L. Danz, D. Simon, S. Barlow, S. R. Marder, and K. Gall, Adv. Funct. Mater. **20**, 162-172 (2010).
31. T. Pretsch, Smart Mater. Struct. **19**, 015006 (2010).
32. Q. Zhao, W. Zou, Y. Luo, and T. Xie, Sci. Adv. **2**, e1501297 **(**2016).

33. J. Zhang, J.-Y. Ou, K. F. MacDonald, and N. I. Zheludev, J. Opt. **14**, 114002 (2012).

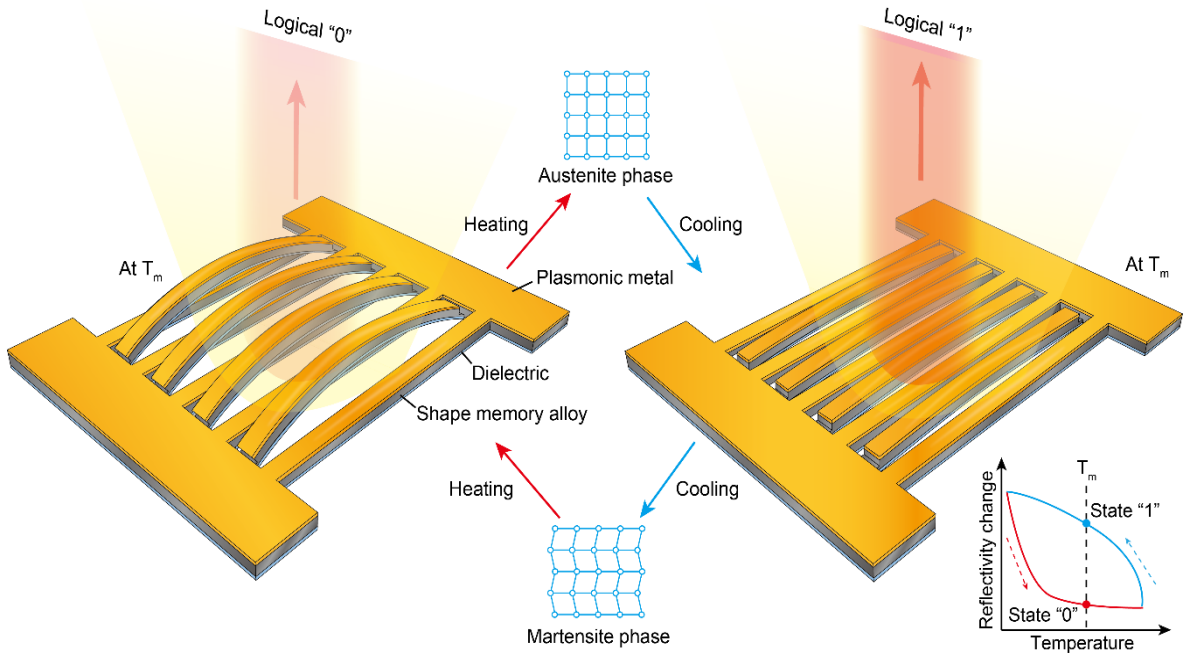

Fig. 1. Shape memory photonic nanostructure. For a given temperature T_m the nanostructure has two different stable shapes as shown, depending on the phase of the NiTi alloy component forming the nanostructural framework. Transition between these shapes can be achieved in a temperature cycle within which NiTi transforms between its martensite and austenite phases in a hysteretic fashion. The change in the shape of the nanostructure leads to a change in its plasmonic response and thereby its optical properties, which are dominated by the gold coating on the NiTi framework. (Note that in these artistic sketches the structural deformation is highly exaggerated and in fact happens at a level comparable to or smaller than the thickness of the nanowires.)

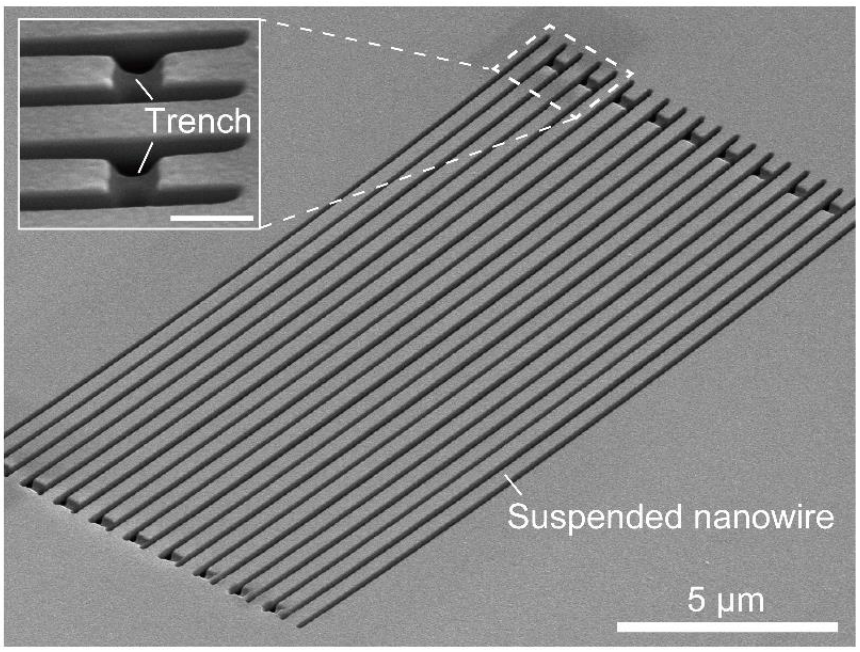

Fig. 2. Shape memory photonic nanowire array. Scanning electron microscope image of the nanostructure fabricated on a Au-NiTi-SiN nano-membrane. The inset shows the trenches fabricated at the ends of every other beam (scale bar = 500 nm).

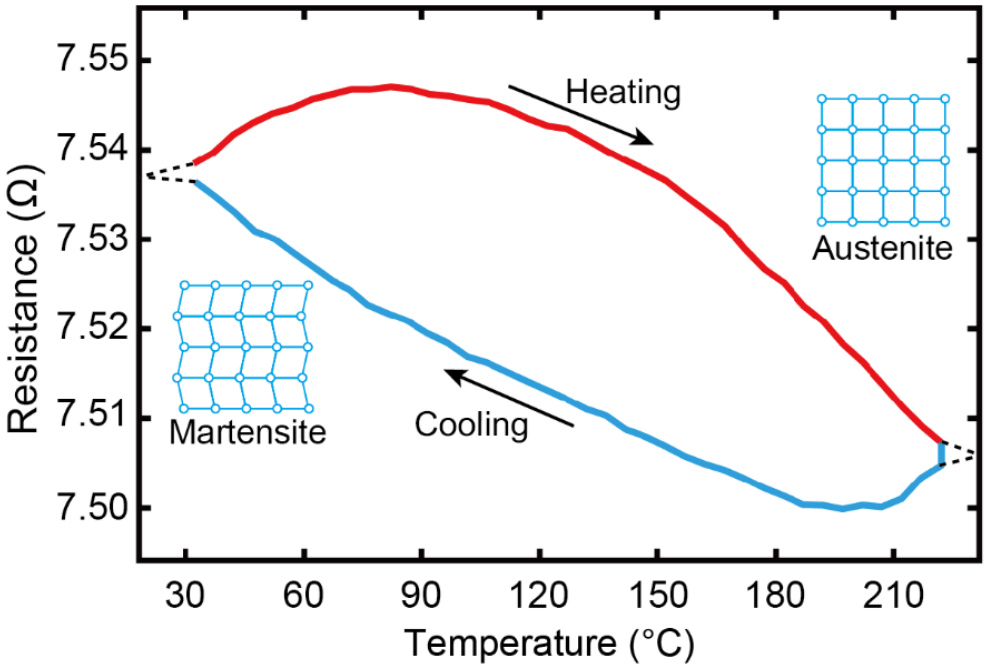

Fig. 3. Hysteretic dependence of resistance on temperature for a 175-nm-thick NiTi film on a fused silica (SiO_2) substrate.

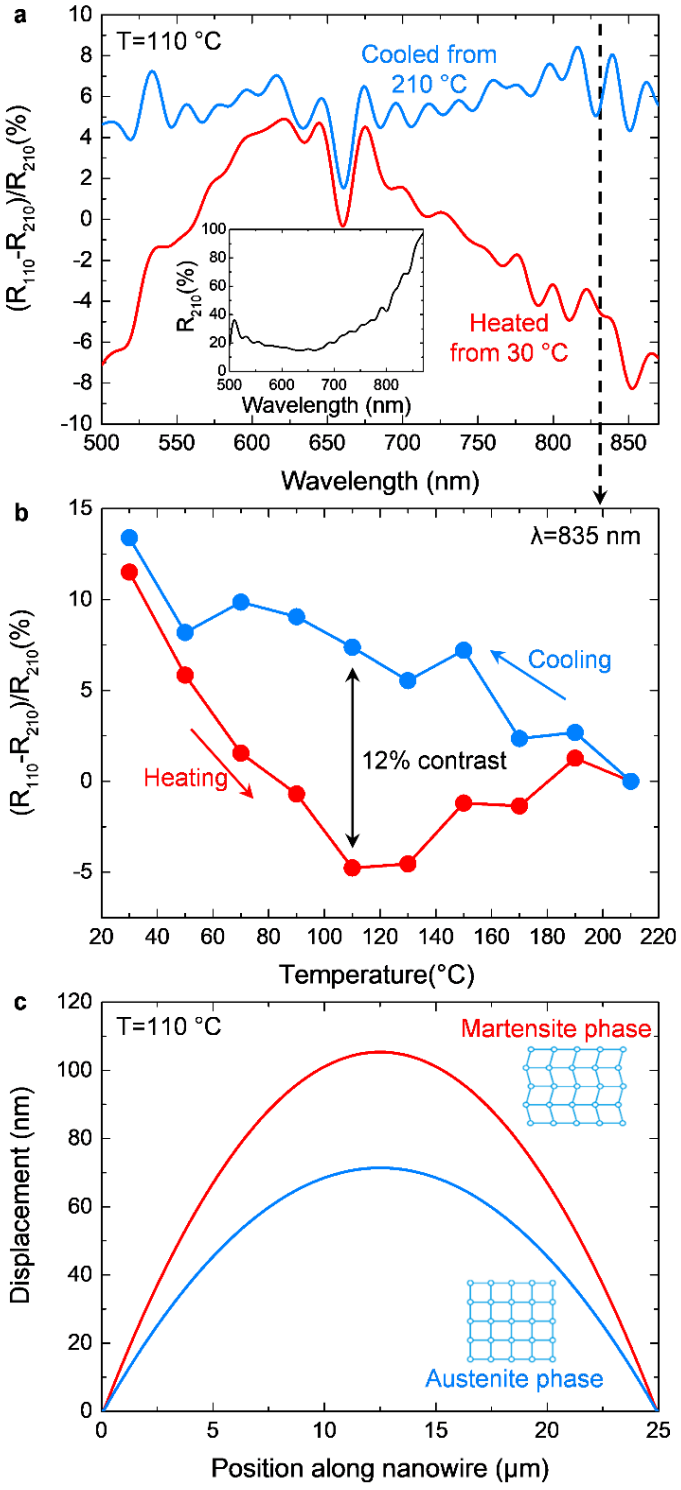

Fig. 4. Deformation-dependent optical properties of the shape-memory nanowire array. (a) Spectral dispersion of the difference between reflectivities of the nanostructure measured at 110°C and 210°C, relative to reflectivity at 210°C. Blue and red curves correspond to the cooling and heating parts of the hysteresis cycle, respectively. The inset shows the reference reflectivity spectrum at 210°C. (b) Difference between the sample reflectivity at temperatures *T* and 210°C relative to the reflectivity level at 210°C at a wavelength of 835 nm. (c) Simulated out-of-plane deformation profile of a nanowire with

trench cuts at each end for NiTi in the martensite (red) and austenite (blue) states at a temperature of 110°C.